Phases of microalgal succession in sea ice and the water column in the Baltic Sea from autumn to spring

Enberg, Sara

2018-07-12

Enberg , S , Majaneva , M , Autio , R , Blomster , J & Rintala , J-M 2018 , ' Phases of microalgal succession in sea ice and the water column in the Baltic Sea from autumn to spring ' , Marine Ecology. Progress Series , vol. 599 , pp. 19-34 . https://doi.org/10.3354/meps12645

http://hdl.handle.net/10138/308486
https://doi.org/10.3354/meps12645

unspecified
acceptedVersion

Phases of microalgal succession in sea ice and the water column in the Baltic Sea from autumn to spring

A running page head: Wintertime microalgal succession in the Baltic Sea

Sara Enberg[1,2,*], Markus Majaneva[1,2,3], Riitta Autio[4], Jaanika Blomster[2] and Janne-Markus Rintala[1,2,5]

[1] Tvärminne Zoological Station, University of Helsinki, J.A. Palménin tie 260, FI-10900 Hanko, Finland

[2] Department of Environmental Sciences, University of Helsinki, P.O. Box 65, FI-00014 Helsinki, Finland

[3] Department of Natural History, NTNU University Museum, Norwegian University of Science and Technology, NO-7491 Trondheim, Norway

[4] Marine Research Centre, Finnish Environment Institute, P.O. Box 140, FI-00251 Helsinki, Finland

[5] INAR – Institute for Atmospheric and Earth System Research, University of Helsinki, P.O. Box 64, FI-00014 Helsinki, Finland

*Corresponding author: Department of Environmental Sciences, University of Helsinki, Viikinkaari 1, P.O. Box 65, FI-00014 Helsinki, Finland. Tel: +358 50 3005447; E-mail: sara.enberg@gmail.com

Abstract

The phytoplankton biomass during the cold-water season (October−May) in the Baltic Sea is low compared to the warm-water season (June–September). However, the sea ice is a habitat for diverse assemblages in polar and subpolar areas. These areas, including the Baltic Sea, are subject to changing environmental conditions due to global warming, and temporal and spatial studies are required to understand changes in the processes organisms are involved in. We delineated the microalgal succession in the northern Baltic Sea during the cold-water season using a weekly collected dataset. The microscopy results together with molecular methods showed that the sea ice microalgal assemblage formed a distinct group compared to four phytoplankton assemblages, and suggested that the cold-water season could be divided to five microalgal groups; sea ice and four phytoplankton assemblages (fall, winter, under-ice water and spring). The microalgal biomass based on cell enumeration in the water column remained low until the end of the ice-covered season and was dominated by small flagellates and dinoflagellates. The young-ice assemblage in January resembled the water column assemblage, but indicated a partly selective species concentrating mechanism during ice formation due to lower species richness in ice compared to the water column. Biomass of microalgae increased in the ice and water columns during the March−May, and the assemblage changed from being flagellate-dominated to being diatom- and dinoflagellate-dominated. In addition, the spring phytoplankton formed, based on species and biomass, a separate assemblage, indicating that sea ice algae did not contribute to the spring bloom phytoplankton assemblage.

Key words: microalgae, cold-water season, succession, sea ice, Baltic Sea

Introduction

Phytoplankton succession studies in the Baltic Sea have focused on the high-growth season (from spring to fall) (e.g. Niemi 1973, Andersson et al. 1996, Klais et al. 2013, Lips et al. 2014, Svedén et al. 2016). The classical temperate phytoplankton succession description begins in spring, when increasing light enhances primary production, and the spring bloom diatoms exhaust nutrients from the water column (Lips et al. 2014). The changes in phytoplankton assemblages follow the changes in the physical environment, i.e. available light and nutrient supply (Popova et al. 2010), but also the species interactions, such as competition and grazing (Sommer et al. 1986). A low-production phase with small flagellated algae follows in the summer, but summertime diazotrophic cyanobacterial blooms are a recurrent phenomenon in eutrophic waters (Finni et al. 2001, Kahru et al. 2007, Svedén et al. 2016). During the fall, when the temperature decreases and stratification is broken, nutrients are replenished and a bloom of diatoms and dinoflagellates may occur (Wassmund & Uhlig 2003). The wintertime in high-latitude seas is characterized by low algal biomass and a predominance of small mixotrophic and heterotrophic taxa (Dale et al. 1999, Moreau et al. 2010, Nicolaus et al. 2012, Krawczyk et al. 2015, Makarevich et al. 2015).

Parallel to the seasonal succession of phytoplankton in high-latitude seas, an annual primary succession occurs in the sea ice, with organisms living in the water column colonizing newly formed sea ice (Lizotte 2003). The initial algal colonization of sea ice has been described as both a non-selective and selective concentrating mechanism during ice formation (Garrison et al. 1983, Ikävalko & Gradinger 1998, Tuschling et al. 2000, Różańska et al. 2008). In laboratory experiments, the transition from an open-water to a sea-ice habitat is characterized by an initial physiological inhibition, which is followed by subsequent adaptation (Grossmann & Gleitz 1993).

Based on time series data, a recent review (Leu et al. 2015) suggested a division of sea-ice assemblages into three functional phases (pre-bloom, bloom and post-bloom) mostly driven by allogenic factors such as temperature and light. Flagellates, likely heterotrophic (Mikkelsen et al. 2008, Różańska et al. 2009), predominate in the pre-bloom. Towards the spring, the increasing solar angle and air temperature diminish the snow cover, increase the ice temperature and enlarge the brine channels (Golden et al. 1998), providing more light and space for ice algae to grow. Photosynthetic diatoms and dinoflagellates dominate in the sea-ice bloom (Stoecker et al. 1992, Gleitz et al. 1998, Ratkova and Wassmann 2005, Mikkelsen et al. 2008). The arborescent colony-forming pennate diatom *Nitzschia frigida* is a key species of land-fast ice across circum-Arctic regions (Syvertsen 1991, Różańska et al. 2009, Poulin et al. 2011). A heterotrophic assemblage characterizes the post-bloom (Haecky and Andersson 1999, Kaartokallio et al. 2008, Riedel et al. 2008). Most of the previous sea ice related research has focused on the bloom and post-bloom assemblages (Stoecker et al. 1993, Sime-Ngado et al. 1997, Kaartokallio 2004, Thomson et al. 2006, Różańska et al. 2009), and little is known of the flagellate-dominated pre-bloom (Niemi et al. 2011).

Furthermore, comprehensive long-term studies are needed to understand the algal processes that occur in various polar marine ecosystems, which are more likely subject to changing environmental conditions due to global warming, especially during the winter season. However, findings that environmental conditions (mainly ice extent; Legrand et al. 2015, Beall et al. 2016) and assemblage composition (Kremp et al. 2008, Majaneva et al. 2012a) during the winter season govern the magnitude and composition of the phytoplankton spring bloom urge for more research. The pelagic and ice-algal assemblages of the Arctic and Antarctic differ from those in the low-salinity Baltic Sea, but the biota originates from the same evolutionary lineages and experience the same physical properties (low light and temperature, salinity) during the winter season, and it is therefore likely that similar phenologies occur.

Our paper describes phytoplankton and sea ice assemblage succession and species dynamics in the water column, under-ice water (UIW) and sea ice during a cold-water and ice-covered season in the northern Baltic Sea. The succession of two different sites is described, with different sea ice cover probabilities, starting from late autumn with open water until the end of the phytoplankton spring bloom. Based on changes in microalgal assemblage composition (microscopy cell enumeration and molecular methods) we divide the cold-water season into different groups based on algal assemblage composition, discuss the interactions among the groups and link the ice algal assemblage with the phytoplankton spring bloom assemblage.

Materials and Methods

Study site and field sampling

Our study was carried out on the northwest coast of the Gulf of Finland, Baltic Sea. Two different locations were selected as study sites. Krogarviken, site A (59° 50.650´ N, 23° 15.100´ E), is a semi-enclosed shallow bay with average water depth of only 3 m. The sitehas high sea-ice probability and events of sea-ice breakups are unlikely during the ice-covered season. Storfjärden, site B (59° 51.250' N, 23° 15.815' E), is approximately 30 m deep and more exposed to heavy winds, which can easily cause sudden sea ice breakups. The sampling was carried out from 8 Oct 2012 to 20 May 2013, with the exceptions of 24 and 31 Dec 2012 and on 22 Apr 2013 when the sea ice started to melt. In addition, due to poor sea-ice conditions, samples could not be collected from site B in 7 Jan 2013, or 11 and 18 Feb 2013.

Three replicate water samples were taken from each site (A: 0–3 m; B 0–15 m) using 3-m and 15-m long hose samplers (6 cm internal diameter). The cutoff of 15 m at site B was chosen as a typical depth scale for the euphotic zone (Luhtala & Tolvanen 2013). The water samples were collected into 2-L transparent plastic bottles without any pre-filtration. After sea ice had formed, three snow thicknesses on the ice were measured from three random spots with 1-cm precision, followed by ice sampling using a motorized CRREL-type ice-coring auger (9 cm internal diameter; Kovacs Enterprises, Roseburg, OR, USA). Sea ice temperatures were measured at 5-cm intervals using a Testo 110 thermometer, and sea ice thicknesses were measured from the obtained ice cores before they were placed in plastic tubing (Mercamer Oy, Vantaa, Finland). Three replicate ice samples were taken from each site. For one replicate ice sample, 2–5 entire ice cores, depending on the ice thickness, were drilled and pooled to ensure enough melted sea ice comparable to the 2-L water samples. In addition, three replicate UIW samples were collected from the drill hole by submerging the 2-L plastic sample bottle under the water's surface. Water temperature and salinity were measured using a Falmouth Scientific NXIC CTD. All of the obtained water and sea ice samples were kept in the dark during transportation to the field station, where the sea ice samples were crushed and melted without allowing the temperature of the sample to rise above +4 °C, as explained in Rintala et al. (2014). The melting method used in this study also avoids salinity shocks in ice algal assemblages which was statistically shown at the same site by Rintala et al. (2014). After this, the ice samples were treated in the same way as the water samples. The bulk salinities of the melted sea ice samples were measured with an YSI 63 meter (Yellow Springs Instruments Inc., Yellow Springs, OH, USA).

Nutrients

For nutrient analysis 1000-mL of water from each three replicates was pooled into one sample. Both inorganic (NH_4, NO_2+NO_3, PO_4, and SiO_4) and total nutrient (tot-N and tot-P) concentrations were determined using a Hitachi U-110 Spectrophotometer (Hitachi High-Technologies Corp., Tokyo, Japan) with standard protocols for seawater analysis (Koroleff 1976). Ice nutrient concentrations were normalized to the mean bulk salinities of melted sea ice to correct for salinity-related variations in the nutrient concentrations.

Chlorophyll *a* measurements

For measuring chlorophyll *a* (chl *a*) concentration, two 100-mL subsamples were taken from every water and ice sample. They were filtered onto GF/F filters (Whatman, Sigma-Aldrich Co. LLC, St. Louis, MO, USA), soaked in 96% v/v ethanol and kept in darkness overnight to extract chl *a* (HELCOM 1988). The chl *a* concentration was calculated from the chl *a* fluorescence measured with a Cary Eclipse spectrofluorometer (Varian Inc. (Agilent Technologies), Santa Clara, CA, USA) calibrated with pure chl *a* (HELCOM 1988). The chl *a* concentrations for ice were converted to mg m^{-3} of sea ice by multiplying the chl *a* concentration of the meltwater by a standard sea ice to seawater density ratio (917 kg m^{-3} / 1020 kg m^{-3} = 0.9) as explained in Meiners et al. (2012).

Microalgal identification, cell enumeration and biomass estimation

For microalgal identification, 200-mL subsamples were collected into brown glass bottles from every sample, preserved with acid Lugol's solution and stored refrigerated in darkness until microscopic enumeration. Only one of the three replicates was used for the microalgal identification, cell enumeration and biomass estimation. Depending on the sample's microalgal density, a volume of 50 mL or 10 mL was settled for 24 h, according to Ütermöhl (1958), and examined with a Leica DM IL, Olympus CK30 or Olympus CKX41 inverted light microscope equipped with 10x oculars and 10x or 40x objectives (Leica Microsystems, Wetzlar, Germany; Olympus Corporation, Hamburg, Germany). More than 50 µm large cells and colonies were counted with 100x magnification over an area covering one half of the cuvette, and the abundance of single-celled and small taxa was counted from 50 random fields with 400x magnification. The species with morphological characteristics visible in an inverted microscope, e.g. with easily recognizable colony structure and cell shape, were identified to the species level, whereas microscopically unidentifiable species were left to a general level. Species easily identified incorrectly (*Gymnodinium corollarium*, *Biecheleria baltica* and *Apocalathium malmogiense*) due to similar gross morphology were identified as the *'Scrippsiella' complex* in the acid Lugol's fixed samples. The cell numbers were converted into carbon biomasses (mg C m^{-3}) using species-specific biovolumes and carbon contents according to Olenina et al. (2006) and Menden-Deuer & Lessard (2000). The biomass was converted to mg m^{-3} of sea ice in a similar manner as the chl *a* concentration used for ice (see above).

DNA isolation and 18S rRNA gene identification

For the DNA extraction, 500 or 1000 mL of water and melted sea ice was sequentially filtered using 47-mm diameter 180-µm pore-size nylon filters (Merck Millipore, Billerica, MA, USA), 20-µm Polyvinylidene fluoride filters (Durapore©, Millipore) and 0.2-µm mixed cellulose ester membrane filters (Schleicher and Schuell Bioscience GmbH, Dassel, Germany). The filters were stored in a -80 °C freezer until further processing. Total DNA was extracted from the 0.2-µm filters using a PowerSoil® DNA Isolation Kit (MO BIO Laboratories Inc., Carlsbad, CA, USA).

PCR amplification was carried out in two stages following Koskinen et al. (2011). In brief, the V4 region of the 18S rRNA gene was amplified, using Phusion polymerase (Finnzymes, Espoo, Finland) and forward primer E572F (Comeau et al. 2011) with truncated Illumina 5' overhang 5'-ATCTACACTCTTTCCCTACACGACGCTCTTCCGATCT-3' and reverse primer 897R (Hugerth et al. 2014) with 5' overhang 5'-GTGACTGGAGTTCAGACGTGTGCTCTTCCGATCT-3'. Cycling conditions consisted of an initial denaturation at 98 °C for 30 s, 20 cycles of 98 °C for 10 s, 65 °C for 30 s and 72 °C for 10 s, and a final extension for 5 min. The amplification was completed in three replicates during the second stage, using a full-length Illumina P5 adapter and Indexed P7 adapters. The replicates were pooled between and after the amplifications. The PCR products were purified using AMPure XP beads (Beckman Coulter Inc., Brea, CA, USA) and quantified with Qubit (Invitrogen, CA, USA). The amplicons were paired-end sequenced on an Illumina MiSeq

instrument using a v3 600-cycle kit (Illumina, CA, USA) at the Institute of Biotechnology (Helsinki, Finland).

The resulting reads were processed, using usearch v8.1.1831_win32 (Edgar 2013). For details of the methods, see Supplementary file 1. In brief, the paired-end reads were merged using -fastq_mergepairs and quality-filtered using a -fastq_filter with a minimum read length of 200 bases and a 1.0 maximum expected error rate. The primer sequences were removed and the reads were dereplicated, using -derep_fulllength. Singletons were removed and operational taxonomic units (OTU) were clustered at a 97% similarity level, using -cluster_otus. The above steps were performed for each sample, and the resulting OTU fasta-files were pooled using merge.files in mothur v.1.36.1 (Kozich et al. 2013). The OTUs were next sorted based on the abundance of reads assigned to them, using usearch command -sortbysize. To remove duplicate OTUs stemming from taxa present in several samples, the merged OTUs were re-clustered at a 97% similarity level, using -cluster_otus -minsize 2. The abundance of each OTU in each sample was resolved, using -usearch_global against the pooled OTU file. This pipeline was developed based on an analysis of a mock assemblage and seven negative PCR reactions sequenced together with the samples (M Majaneva unpubl. data). The identity of the 97% OTUs was searched, using classify.seqs in mothur against the PR^2 reference library (Chevenet et al. 2006, Chevenet et al. 2010, Guillou et al. 2013) and using blastn search in BLAST 2.3.0+ (Zhang et al. 2000) against a nucleotide database at the National Center for Biotechnology Information (NCBI), followed by the lowest common ancestor algorithm in MEGAN6 (minimum bit score 400, top percentage 3.0 and minimum support 1; Huson et al. 2016). Taxonomy was assigned based on an agreement between the two searches. In the absence of a taxonomic assignment, the OTU was treated as unclassified and removed from further analyses as a putative chimera (372 OTUs).The OTUs assigned as Metazoa, land plants and land fungi were also removed for the downstream analyses (41, 10 and 38 OTUs, respectively), and the number of reads/sample was normalized to 27591. Diversity metrics (ACE, Shannon and inverse Simpson's indices based on OTU abundance) were calculated, using the summary.single command in mothur. The raw reads were submitted to the Sequence Read Archive of the European Nucleotide Archive's (ENA) with accession number PRJEB21047 (work in progress, not yet public).

Statistical methods

One-way analysis of variance (ANOVA) was used to test the significance of the differences between the sites and between ice and water for chl *a* and diversity metrics. Levene's test was used to test the homogeneity of variances and Shapiro-Wilk test to test the assumption of normality of the data.The significance level $p < 0.05$ was used for both tests. A parametric ANOVA and Tukey's b test in pairwise comparisons were used when the variances were homogenous, while a non-parametric Kruskal-Wallis test with ranked data and the Mann-Whitney U test were used when the variances were unequal. The correlation between algal biomass and chl *a* concentrations was analysed with Spearman's rank-order correlation. For all the tests, $p < 0.05$ was considered statistically significant. The procedures were performed in SPSS for Windows (version 23, IBM SPSS Statistics 2015; IBM Corp., Armonk, NY, USA).

To divide assemblages from the OTU and microscopy analyses into different groups, the PRIMER v6.1 package of the Plymouth Marine Laboratory and the programme PAST 3.04 (Hammer et al. 2001) were used to perform the multivariate analyses (71 samples). Microalgae and OTUs observed more than once in at least two samples were included in the analyses to ensure sufficient data for ordination, thus reducing the total number of taxa from 76 to 40 (microalgae) and from 1137 to 661 (OTUs). Data on algal biomasses and OTU abundance were log(x+1) transformed to produce a less severe transform for small values. Groups were defined *a priori* based on substrate and time (water-ice, fall-winter-spring) and hierarchical cluster analysis was conducted on the taxon composition

between the samples (Bray-Curtis' similarity index) and tested for significant differences using one-way PERMANOVA with 9999 permutations (Anderson 2001).

Results

Environmental dynamics

Winter 2012–2013 was characterized by long-lasting ice cover, lasting from mid-December to mid-April on the coast of the Gulf of Finland (http://en.ilmatieteenlaitos.fi/ice-winter-2012-2013). The thermal winter (the daily mean temperature remains below 0°C) began on 29 Nov 2012 in the sampling area and ended 11 Apr 2013. A short warm period occurred between 27 Dec 2012 and 4 Jan 2013, during which the mean temperature was above 0 °C. The heaviest rains were observed during October–December, and snow cover was permanent from 29 Nov 2012 until 18 Apr 2013 (Fig. S1 in the Supplement).

At the beginning of our study, the water column was mixed and the temperature was approximately +11 °C at both sites. The temperature decreased towards ice formation, and the temperature was close to zero degrees throughout the water column during the ice-covered season. After ice melt, the water temperature increased, and on 20 May 2013 thermal stratification was established at both sites (Fig. S2). Before ice formation, the salinity was approximately 5.5 at site A and 6.0 at site B. Salinity decreased during the ice-covered season, and was 3.5–5 at site A and 4.7–5.7 at site B. After ice breakup, the salinity was higher compared to the ice-covered season (4.6–5.6 at site A and 5.5–5.9 at site B) (Fig. S3).

The ice conditions differed between the two sites. The ice-cover at site A formed at the end of 2012 and broke up after mid-April 2013. The first ice samples were collected on 7 Jan 2013, when ice thickness was 9 cm. A maximum ice thickness of 47 cm was reached at the beginning of April (Fig. 1a). The first ice samples from site B were collected on 14 Jan 2013, when ice thickness was 11 cm. The weather conditions changed in mid-February, and strong winds broke up the ice. Samples were collected again on 28 Feb 2013, when the ice field was reformed from old ice floes either singly or by being packed on top of each other. There was also new ice that had formed between the old ice floes, but this ice was not sampled. The ice reached a maximum thickness of 53 cm at the end of March, and site B was ice free in mid-April one week prior to site A (Fig. 1b). Snow cover thickness varied between 0–19 cm and 0–3 cm at sites A and B, respectively (Fig. 1).

The concentrations of NH_4-N, NO_2+NO_3-N, PO_4-P, SiO_4-Si and total N and P concentrations in the ice were lower compared to those in the water column, except for NH_4-N, which was higher in the ice and UIW compared to the 0–3-m and 0–15-m layers at sites A and B, respectively. After ice breakup the PO_4-P and SiO_4-Si concentrations decreased in the water column and NO_2+NO_3-N concentration was zero. The total N and P concentrations showed a small decrease after ice breakup (Table S1 in the Supplement).

Seasonal dynamics of chl *a* and the microalgal assemblages

The chl *a* concentration in the water column was low from the beginning of the study until April, and the maximum concentration was 6 mg chl *a* m^{-3} at both sites (Fig. 2). The ice chl *a* concentration differed significantly between the two sites throughout the ice-covered season (Kruskal-Wallis test, Mann Whitney U test, all $p < 0.05$). The chl *a* concentration in the ice at site A increased from 4.4 ± 0.3 mg chl *a* m^{-3} at the beginning of the ice-covered season to 32.0 ± 3.8 mg chl *a* m^{-3} by 8 Apr 2013, after which the chl *a* concentration decreased in the ice and subsequently increased in the UIW and 0–3-m layer. The highest ice chl *a* concentration at site B (18.9 ± 1.8 mg chl *a* m^{-3}) was observed on 28 Feb 2013, after reformation of the ice field. After 28 Feb 2013, the ice chl *a* concentration decreased towards ice breakup, and was 6.5 ± 0.4 mg chl *a* m^{-3} on 8 Apr 2013. Although the chl *a* concentration at site B increased in the UIW and 0–15-m layer during the

spring, the maximum concentration was similar to that in the ice. During the phytoplankton spring bloom, between 13 and 20 May 2013, the chl *a* concentration was significantly higher in the water column at site A than at site B (Kruskal-Wallis test, Mann Whitney U test, all $p < 0.05$) (Fig. 2).

Similar to the chl *a* concentration, total biomass of microalgae based on cell enumeration was low in the water column throughout the cold-water season. The total microalgal biomass at the beginning of the study was 80 mg C m^{-3} at both sites, and decreased to less than 10 mg C m^{-3} during December (Fig. 3). The total biomass in the ice was higher compared to the water column from the beginning of February at site A and after 28 Feb 2013 at site B until 8 Apr 2013 (Fig. 3). The total biomass of microalgae in the ice differed between the two sites throughout the ice-covered season (January–mid-April). Total biomass in the ice at site A was 42−98 mg C m^{-3} in January and increased to 240 mg C m^{-3} on 28 Feb 2013. The total biomass of microalgae in the ice decreased during March, but increased again in April and highest total biomass (280 mg C m^{-3}) was observed 2 Apr 2013 at site A. Total biomass of microalgae in the ice at site B was below 40 mg C m^{-3} in January and February before the ice breakup. Highest total biomass in ice (290 mg C m^{-3}) was observed 28 Feb 2013 after the reformation of ice, after which the total biomass in ice first decreased and then increased again towards the final ice breakup. An under-ice phytoplankton bloom was observed at both sites in April, and the total biomass in the UIW was 400 mg C m^{-3} and 500 mg C m^{-3} at sites A and B, respectively. During the phytoplankton spring bloom, the total biomass varied between 200 and 500 mg C m^{-3} and 250 and 350 mg C m^{-3} at sites A (layer 0−3 m) and B (0−15 m), respectively (Fig. 3). Total biomass correlated positively with the chl *a* concentration (Spearman's rank-order correlation, n=109, r=0.822, p=0.01).

Light microscopy

A total of 76 taxa were identified from the samples with inverted light microscopy (Table S2). At the beginning of our study, the algal biomass in the water column was dominated by dinoflagellates (37–68 %), cryptophytes (8–11 %) and other small flagellates (16–29 %) identified as classes Prymnesiophyceae (*Chrysochromulina birgeri*) and Prasinophyceae (*Pyramimonas* sp.) in addition to small unidentified flagellates (Fig. 4e and f). *Heterocapsa triquetra*, *Dinophysis* sp. and the *'Scrippsiella' complex*'Scrippsiella' complex were abundant dinoflagellates, but most dinoflagellates were unidentifiable. Diatoms, both centric (e.g. *Chaetoceros* sp., *Skeletonema* spp.) and pennate (e.g. *Pauliella taeniata* and *Navicula* sp.) and filamentous cyanobacteria (*Planktothrix* sp. and *Aphanizomenon* sp.) were present at both sites. Despite the decreasing biomass during October–December, the algal assemblage in the water column at the beginning of the ice-covered season (7 and 14 Jan 2013) resembled the fall assemblage and was dominated by dinoflagellates (30–48 %), cryptophytes (~20 %) and small unidentified flagellates (28–35 %) (Fig. 4e and f). The UIW assemblage was also dominated by dinoflagellates (38–73 %), cryptophytes (11–14 %) and small unidentified flagellates (14–43 %) (Fig. 4c and d).

The ice was characterized by low biomass at the beginning of the ice-covered season (7 Jan 2013 – 14 Feb 2013), and the ice algal assemblage resembled the water column assemblage, but the two sites differed. In January, the assemblage at site A was dominated by dinoflagellates (10–32 %), especially unidentified dinoflagellates and the *'Scrippsiella' complex*. Other abundant microalgae were cryptophytes (12–22 %), small flagellates (19–41 %) and cyanobacteria (10–29 %) (Fig. 4a). Green algae increased in February, especially *Chlamydomonas caudata* and *Klebsormidium flaccidum* and the euglenophytes. At site B, the assemblage in January was dominated by dinoflagellates (28–65 %), especially unidentified dinoflagellates and small flagellates (13–43 %). Cryptophytes, cyanobacteria, green algae and euglenophytes were present, but their biomasses were lower compared to site A (Fig. 4b). At the end of February, the ice shifted from winter to spring ice, which was characterized by an increase in algal biomass and change in assemblage composition towards the predomination of diatoms and dinoflagellates (Fig. 4a and b). At site A, green algae,

dominated by *Klebsormidium flaccidum*, was the third largest group (22–47%) along with diatoms (11–50%) and dinoflagellates (7–50%). At site B, small flagellates remained the third largest group (13–36%) along with diatoms (30–63%) and dinoflagellates (13–49%) (Fig. 4a). The biomass of *Heterocapsa arctica* sub. *frigida* increased, but the dinoflagellate assemblage was dominated by unidentified dinoflagellates and the *'Scrippsiella' complex*. The ice diatom assemblages at both sites were dominated by pennate species including cell chains forming *Pauliella taeniata*/*Navicula* sp. and arborescent colony-forming *Nitzschia frigida*. The centric diatoms were present in the ice throughout the study, but the biomass of centric diatoms, especially from the genera *Chaetoceros* and *Melosira*, increased before ice breakup.

The biomass of dinoflagellates increased in mid-March, and dinoflagellates dominated the algal assemblage in the water column (57–81%) (Fig. 4e and f) and UIW (57–76%) (Fig. 4c and d). The most dominant dinoflagellates were unidentified dinoflagellates, species from the *'Scrippsiella' complex* and *Peridiniella catenata*. Diatom biomass increased in April, when diatoms formed 8–36% and 5–30% of the algal biomass in the water column and UIW, respectively. The most abundant diatoms were *Skeletonema* spp., *Chaetoceros* sp. and *Pauliella taeniata*/*Navicula* sp.

The spring bloom assemblage was dominated by dinoflagellates (20–66%) and diatoms (28–80%) after ice melt (29 Apr 2013 – 22 May 2013) at both sites (Fig. 4e and f). The unidentified dinoflagellates, *'Scrippsiella' complex*, *Peridiniella catenata* and *Protoperidinium* sp. dominated the dinoflagellates during the spring bloom. The diatom species *Pauliella taeniata*/*Navicula* sp. abundant in the water column and UIW before ice breakup was present in the spring bloom with low abundances. *Skeletonema* spp. dominated the diatom assemblage at the beginning of the spring bloom. Later, the diatom assemblage was dominated by the pennate diatom *Diatoma tenuis*.

Taxonomic affiliation of sequences

The taxa identified with light microscopy contributed only a small portion of the OTUs detected in the samples: the sequence data from 58 samples yielded 1039 OTUs at a 97% similarity level. The OTU number varied between samples, being 69–259 (mean ± standard deviation = 172 ± 50) per sample. The taxonomic distribution of OTUs assigned showed that the main groups present at both sampling sites were ciliates, fungi, dinoflagellates, cercozoa, green algae and stramenopiles, a divergent group that includes e.g. diatoms, chrysophytes, bolidophytes, eustigmatophytes, dichtyochophytes and pelagophytes (Fig. S4a–f). Here, we concentrate on the predominant dinoflagellates, green algae, diatoms, cryptophytes and haptophytes (Fig. 5a–f). Although mainly phototrophic, these groups may also include mixotrophic, phagotrophic or parasitic species, e.g. certain dinoflagellate species from genus *Gyrodinium* and cryptophytes from genus *Goniomonas*.

Dinoflagellates were the OTU-richest phototrophic group in October–December (with a mean of 34 OTUs in the samples), followed by green algae (20), chrysophytes (15), diatoms (19), cryptophytes (14) and haptophytes (5) (Fig. S4e and f). The most abundant dinoflagellate OTUs were affiliated with *Heterocapsa triquetra*, *Prorocentrum* sp. and unassigned dinoflagellates. For green algae, *Nannochloris* sp. and *Choricystis* sp. OTUs predominated. The most abundant diatom OTUs were affiliated with centric diatoms and belonged to genera *Thalassiosira*, *Chaetoceros* and *Skeletonema*. The most abundant cryptophyte OTUs were affiliated with *Falcomonas daucoides*, *Teleaulax acuta* and unassigned cryptophytes, while the most abundant haptophyte OTU was affiliated with *Chrysochromulina birgerii*. Despite the diminishing biomass and changes in assemblage composition, the OTU-based diversity was stable between October and December (repeated-measures ANOVA, $p > 0.05$), and the diversity was higher compared to the water column during January–May (Fig. 6a).

An average of 18 dinoflagellate OTUs were collected from the water column samples (Fig. S4c–f) during the ice-covered season (7 Jan 2013 – 15 Apr 2013), and the most abundant OTUs were affiliated with *Gyrodinium* sp., *Prorocentrum* sp., *Heterocapsa triquetra* and unassigned dinoflagellates. The mean number of dinoflagellate OTUs in the sea ice samples was seven (Fig. S4a and b), and the most abundant OTUs were *Gymnodinium* sp. (*G. dorsalisulcum*), *Apocalathium malmogiense* in addition to *Heterocapsa triquetra* and unassigned dinoflagellates. The mean number of diatom OTUs in the water column was 15 (Fig. S4c–f), and the most abundant species were centric diatoms *Thalassiosira guillardii*, *T. hispida*, *Skeletonema* sp. (*S. marinoi*), unassigned Coscinodiscophyceae and pennate *Cymbella* sp. The mean number of diatom OTUs in sea ice was 13 (Fig. S4a and b), and the centric diatom *Chaetoceros socialis* and unassigned Coscinodiscophyceae were the most abundant OTUs. The mean number of green algae OTUs was 17 and 14 in the water column and ice, respectively (Fig. S4a–f), and *Chlamydomonas* sp. was abundant especially in the UIW and sea ice. The mean number of cryptophyte OTUs was 11 in both the water column and the UIW (Fig. S4c–f), and the most abundant OTUs were affiliated with *Teleaulax acuta* and unassigned cryptophytes. The sea ice had an average three cryptophyte OTUs (Fig. S4a and b), and *Chroomonas* sp. and *Falcomonas daucoides* were the most abundant OTUs. Both the UIW and water column averaged five haptophyte OTUs (Fig. S4c–f), while sea ice only averaged three OTUs (Fig. S4a and b), and similar to the October–December period, the most abundant OTU was *Chrysochromulina birgerii*. The diversity of the water column assemblage during the ice-covered season (7 Jan 2013 – 15 Apr 2013) was lower compared to the water column during October–December, and the diversity in UIW was lower than that in the water column during the ice-covered season (Fig. 6a). OTU-based richness in sea ice was lower compared to the water column and UIW. Evenness, however, was the highest in sea ice (Fig. 6b). Evenness increased during the ice-covered season, especially at site B.

The mean number of dinoflagellate OTUs was 10 during the spring bloom (29 Apr 2013 – 22 May 2013) (Fig. S4e and f), and unassigned dinoflagellates were the most abundant, in addition to *Gymnodinium dorsalicum*, which was abundant at site A. The mean number of diatom OTUs was 16 (Fig. S4e and f), and the most abundant species were the centric diatoms *Chaetoceros* sp. (*C. socialis*), *Thalassiosira guillardii*, *T. hispida*, *Skeletonema* sp. (*S. marinoi*) and the pennate diatom *Cymbella* sp. The mean number of cryptophyte OTUs was seven (Fig. S4e and f), and the assemblage resembled the UIW assemblage, the abundant species being *Falcomonas daucoides*, *Teleaulax acuta*, *Chroomonas* sp. and unassigned cryptomonadales. The mean number of haptophyte OTUs was four (Fig. S4e and f), and the abundance of *Chrysochromulina* sp. decreased. OTU-based richness increased in spring but, typical for a bloom situation, the evenness of the spring water assemblage was low (Fig. 6a and b).

Groups

The dendrogram produced from the Bray-Curtis similarity coefficients for the OTUs (size fraction 0.22–20 µm) showed eight clusters at ~58% similarity (Fig. 7a). The clusters followed the *a priori* groups: the fall (8 Oct 2012 – 17 Dec 2012), the water column during the ice-covered season (7 Jan 2013 – 15 Apr 2013), the UIW (7 Jan 2013 – 15 Apr 2013), the ice (7 Jan 2013 – 15 Apr 2013) and the spring bloom (29 Apr 2013 – 22 May 2013), and the groups harboured significantly different assemblage compositions (one-way PERMANOVA $F = 22.76_{4,54}$, sum of squares = 12.04, within group sum of squares = 5.062, $p < 0.001$). Three extra clusters included five transitional samples: two early UIW samples, two early sea ice samples and one water sample from the winter-spring transition (C14, F14, D13, D14 and F26 in Fig. 7a). In addition, the three first UIW samples (F12, C13, F13 in Fig. 7a) clustered with the winter water samples and the three final winter water samples (A25, E25, E26 in Fig. 7a; sampled under ice) clustered with an early spring water sample.

The dendrogram based on the microalgal biomasses (including microalgae > 20 µm) showed similar clustering as that based on the OTUs (Fig. 7b), and the *a priori* groups based on biomasses harboured significantly different assemblage compositions, except fall and winter water (one-way PERMANOVA $F = 10.23$, sum of squares = 12.26, within group sum of squares = 7.572, $p < 0.001$, Bonferroni corrected). Though the differences between the groups were not as clear based on the algal biomass results as they were for the OTU results, the similarity matrixes (used for producing the dendrograms) were related ($\rho = 0.5$, $p < 0.01$).

Discussion

Our results provide new insight on cold-water season algal succession in the northern Baltic Sea. The temperature and light environment of Baltic Sea differ from those in polar areas. In our study we distinguished five different groups in the microalgae assemblages, four in the water column and one in the sea ice, from the beginning of October throughout the ice-covered season until the end of May, with significant differences in assemblage composition and diversity. Four of the five groups i.e. the fall (8 Oct 2012 – 17 Dec 2012), the water column, the UIW, and the ice during the ice-covered season (7 Jan 2013 – 15 Apr 2013) and the spring (29 Apr 2013 – 22 May 2013) were observed in the water column. The phytoplankton succession in the water column during the cold-water season in our study coincided with changes in light environment and temperature. The algal assemblage composition of the Baltic Sea changes along a salinity gradient (Gasiūnaitė 2005, Ulanova et al. 2009, Sildever et al. 2015), indicating that salinity is also a potential factor shaping the seasonal algal assemblage succession during the cold-water season between ice and water column. For example, the seasonal cyanobacteria succession in the water column correlates with both salinity and temperature (Bertos-Fortis et al., 2016), showing that many of the processes affecting microbial assemblages are complex.

At the beginning of October, the assemblage in the water column was dominated by dinoflagellates and other small flagellates belonging to green algae, cryptophytes and haptophytes. Autumnal succession studies from the Baltic Sea are sparse, but an early autumnal bloom dominated by diatoms (dominated by *Chaetoceros* sp. and small cells of *Thalassiosira* spp.) (Bianchi et al. 2002) or small colonial cyanobacteria (Wasmund et al. 2001) was not observed in our study. The amount of light and temperature decreased during the fall, and changed the physical environment resulting in decreased phytoplankton biomass. After the ice formation small flagellates dominated the algal assemblage in the under-ice water column in concordance with previous wintertime studies (Smith et al. 1991, Clarke & Leakey 1996, Fiala et al. 1998, Ratkova et al. 1998). Flagellate dominance continued until the end of February, probably due to the flagellates' ability to supplement or substitute photosynthesis via mixotrophy and/or heterotrophy as proposed by Mikkelsen et al. (2008).

Różańska et al. (2008) found that nearly every species was observed in both the newly formed sea ice and water column, while only a few species were found exclusively in the water column. In contrast, Tuschling et al. (2000) and Majaneva et al. (2012b) have shown sea ice assemblages to differ from those observed in the water column and in the newly formed sea ice. The sea ice algal assemblage in our study resembled the water column assemblage at the beginning of the ice-covered season and, similar to the water column, was dominated by small flagellates. The lower richness observed in the ice in January compared to the water column -based on the OTUs indicates that ice assemblage formation was not unequivocally a non-selective concentrating mechanism during ice formation, as earlier proposed by Garrison et al. (1983), but that each species in the water column was unable to colonize the forming sea ice. However, the selection of diatoms during ice formation into ice, earlier shown by Gradinger & Ikävalko (1998), was not observed in our study, possibly due to the low diatom abundance in the water column. In situ ice formation studies are challenging in practice, and consequently, as the first ice samples are typically collected days or

weeks after ice formation. This is also true for our study. The characteristics of the algal assemblage during ice formation in this study cannot be determined due to possible changes in the assemblage between ice formation and the first sampling.

The succession of the ice algae observed in our study was similar to the succession described in previous studies beginning with a winter stage with low production, followed by a growth phase and later the melting period, which ends in ice breakup (Haecky & Andersson 1999, Kaartokallio 2004, Granskog et al. 2006, Leu et al. 2015). The low ice algal biomass at the beginning of the ice-covered season has previously been observed in short-term studies performed in the northern Baltic Sea (e.g. Niemi & Åström 1987, Kangas et al. 1993, Piiparinen et al. 2010, Rintala et al. 2010). The algal biomass began increasing towards the spring equinox, and the assemblage changed from a flagellate-dominated assemblage to a dinoflagellate- and diatom-dominated assemblage, showing that early-winter successional species are eliminated by late-winter successional species. The abundant species in the spring ice originated from the initial ice assemblage. The new algal populations could also have been introduced from the UIW due to 1) the upward flux of UIW into the brine channels (Stoecker et al. 1993 and 1998), 2) via the UIW microalgae attaching and accumulating to the bottom-ice surface and ultimately freezing into the ice (Syvertsen 1991) or 3) via a combination of both processes.

Spatial differences between the ice algal assemblage compositions were encountered between the study sites already from the beginning of our study. The biomass of the green alga *Klebsormidium flaccidum*, which lives on rocks and other substrates, was higher at site A compared to site B, indicating that the incorporation of bottom-dwelling species into the ice is more likely in shallow areas. Dinoflagellate cysts are abundant in Arctic and Antarctic sea ice, (e.g. Stoecker et al. 1998, Różańska et al. 2008). Dinoflagellate cysts are numerous in the surface sediment of the Baltic Sea (0–5 cm) (Sildever et al. 2017), but less is known about the dinoflagellate cysts in Baltic Sea ice. Although dinoflagellates dominated the sea ice assemblage in our study, the biomass of dinoflagellate cysts accounted for only a small proportion of the total biomass. Previous studies have shown a low cyst-forming dinoflagellate diversity between the salinities of 6–10 compared to high diversity when the salinity level approaches 30 (Ellegaard 2000, Sildever et al. 2015), indicating that cyst formation is only a minor survival strategy for dinoflagellates in northern Baltic Sea ice, where the salinity is lower compared to oceanic sea ice.

The decrease in ice algal biomass during the end of March and in the beginning of April was followed by a subsequent increase of microalgal biomass in UIW. In concordance with a previous study from the Arctic (Arrigo et al. 2014), the dominant species differed in the water column and to the ice, indicating that the under-ice bloom was formed of species able to reproduce in the UIW environment and not of the dominant sea ice algae. After ice breakup the subsequent phytoplankton bloom and nitrogen depletion were observed in the water column in concordance with previous studies (e.g. Michel et al. 1993, Kuosa et al. 1997, Haecky et al. 1998, Różańska et al. 2009, Sukhanova et al. 2009, Hodal et al. 2012, Lips et al. 2014), but the intensity of the bloom differed between the sites. The assemblage was dominated by diatoms and dinoflagellates during both spring ice and spring bloom, indicating the seeding effect from the sea ice. However, the multivariate analyses showed that species composition was different in the ice compared to the spring bloom, indicating that the spring bloom species were pioneer species of the open-water season. Consequently, as previously suggested by Mikkelsen et al. (2008) and Riaux-Gobin et al. (2011), the spring bloom assemblage was not exclusively formed from sea ice algae, or at least not from the same dominant species. However, Kremp et al. (2008) have shown that the size of inoculum dinoflagellate population and the co-occurring diatoms affects the bloom formation and dominance of the dinoflagellate population. The ice algae released from the melting sea ice, which do not contribute to production in the water column, are grazed by pelagic or benthic herbivores.

Alternatively, the cells could be exposed to microbial degradation or sedimentation, depending on how well the microalgae maintain their buoyancy in the water column. Padisák et al. (2003) showed that the sinking rate is enhanced in colonial-forming microalgae that lack the symmetric shape of the colony. This could explain the decrease of the arborescent colonies of *Nitzschia frigida* after ice breakup. Elimination by immediate cell lysis due to osmotic shock (Garrison & Buck 1986) is unlikely, especially in the Baltic Sea, as Rintala et al. (2014) have shown that direct melting of the Baltic Sea does not cause instant destruction of algal cells.Mild winters are occurring more frequently in the Baltic Sea, and the length of the ice season has decreased by 30 days during the last hundred years (Merkouriadi & Leppäranta 2014). Winters with no ice cover, and experiencing a decrease in salinity and an increase in sea surface temperatures could lead to earlier phytoplankton blooms with increased biomass and smaller phytoplankton taxa, changes that are similar to those described in mesocosm experiments (e.g. Sommer et al. 2007, Winder et al. 2012). A decrease in fresh water ice cover additionally results in a shift from a phytoplankton assemblage dominated by filamentous diatoms to smaller cells (Beall et al. 2016). Ice algal production is estimated to constitute 0.4% of the annual primary production in the Baltic Sea (Haecky & Andersson, 1999). Our results show that ice microalgal biomass base on cell enumeration is high compared to phytoplankton biomass, especially at the end of the ice-covered season. However, if ice thickness is less than 0.5 m, as in our study, the contribution of ice algae to the total primary production remains low (data not shown). In polar areas where ice cover is thicker, the ice algae may contribute more than 50% to total primary production (Gosselin et al. 1997).

In conclusion, albeit the low algal biomass, the cold-water season is a dynamic season with various algal assemblages in the sea ice and water column. The sea ice assemblage resembles the water column assemblage, but species richness was lower in the sea ice compared to the water column, indicating that the formation of the ice assemblage was unlikely a non-selective concentrating mechanism during ice formation. Both the water column assemblage and the sea ice assemblage changed from flagellate-dominated assemblages to diatom-dominated assemblages. However, the sea ice assemblage formed a significantly different group compared to the water assemblages. In addition, the difference between ice and spring bloom assemblage compositions indicates that sea ice algae do not have a large seeding effect from the ice. Although the sea ice assemblage does not greatly contribute to water column phytoplankton growth and spring bloom subsequent to the ice melt, it may contribute greatly to total microalgal biomass during the ice-covered season.

Acknowledgements

The Walter and Andrée de Nottbeck Foundation and University of Helsinki three-year research grants (Blomster) provided financial support for this work. The field and laboratory work was made possible by the facilities at Tvärminne Zoological Station and the Department of Environmental Sciences, University of Helsinki and the Marine Research Centre, Finnish Environment Institute. We thank Göran Lundberg, Veijo Kinnunen and Dr. Joanna Norkko for their help in the fieldwork and Mona Aweys for her help in the DNA extractions. Veijo Kinnunen, Mikael Kraft and Jani Ruohola are acknowledged for their help in the microscopy work. In addition, we would like to thank anonymous reviewers for their valuable comments for the manuscript.

References

Anderson MJ (2001) A new method for non-parametric multivariate analysis of variance. Austral Ecol 26: 32–46.

Anderson MJ, Robinson J (2003) Generalized discriminant analysis based on distances. Aust Nz J Stat 45: 301–318.

Anderson MJ, Willis TJ (2003) Canonical analysis of principal coordinates: a useful method of constrained ordination for ecology. Ecology 84: 511–525.

Andersson A, Hajdu S, Haecky P, Kuparinen J, Wikner J (1996) Succession and growth limitation of phytoplankton in the Gulf of Bothnia (Baltic Sea). Mar Biol 126: 791–801.

Arrigo KR, Perovich DK, Pickart RS, Brown ZW, and others (2014) Phytoplankton blooms beneath the sea ice in the Chukchi Sea. Deep-Sea Res Pt II 105: 1–16.

Beall BFN, Twiss MR, Smith DE, Oyserman BO and others (2016) Ice cover extent drives phytoplankton and bacterial community structure in a large north-temperate lake: implications for a warming climate. Environ Microbiol 18: 1704–1719.

Bertos-Fortis M, Farnelid HM, Lindh MV, Casini M and others (2016) Unscrambling cyanobacteria community dynamics related to environmental factors. Front Microbiol 7: 625, doi: 10.3389/fmicb.2016.00625

Bianchi TS, Rolff C, Widbom B, Elmgren R (2002). Phytoplankton pigments in Baltic Sea seston and sediments: seasonal variability, fluxes, and transformations. Estuar Coast Mar Sci 55: 369–383.

Chevenet F, Brun C, Bañuls AL, Jacq B, Christen R (2006) TreeDyn: towards dynamic graphics and annotations for analyses of trees. BMC Bioinformatics 7: 439.

Chevenet F, Croce O, Hebrard M, Christen R, Berry V (2010) ScripTree: scripting phylogenetic graphics. Bioinformatics 26:1125–1126.

Clarke A, Leakey RJG (1996) The seasonal cycle of phytoplankton, macronutrients, and the microbial community in a nearshore Antarctic marine ecosystem. Limnol Oceanogr 41: 1281–1294.

Comeau AM, Li WKW, Tremblay J-E, Carmack EC. Lovejoy C (2011) Arctic Ocean Microbial Community Structure before and after the 2007 Record Sea Ice Minimum. PLoS One 6: e27492.

Dale T, Rey F, Heimdal BR (1999) Seasonal development of phytoplankton at a high latitude oceanic site. Sarsia 84: 419–435.

Edgar RC (2013) UPARSE: highly accurate OTU sequences from microbial amplicon reads. Nat Methods 10: 996–1000.

Ellegaard M (2000) Variations in dinoflagellate cyst morphology under conditions of changing salinity during the last 2000 years in the Limfjord, Denmark. Rev Palaeobot Palyno 109: 65–81.

Fiala M, Kopczynska EE, Jeandel C, Oriol L, Vetion G (1998) Seasonal and interannual variability of size-fractionated phytoplankton biomass and community structure at station Kerfix, off the Kerguelen Islands, Antarctica. J Plankton Res 20: 1341–1356.

Finni T, Kononen K, Olsonen R, Wallström K (2001) The history of cyanobacterial blooms in the Baltic Sea. Ambio 30: 172–178.

Garrison DL, Ackley SF, Buck KR (1983) A physical mechanism for establishing algal populations in frazil ice. Nature 306: 363–365.

Garrison DL, Buck KR (1986) Organism losses during ice melting: a serious bias in sea ice community studies Polar Biol 6: 237–239.

Gasiūnaitė ZR, Cardoso AC, Heiskanen A-S, Henriksen P and others (2005) Seasonality of coastal phytoplankton in the Baltic Sea: Influence of salinity and eutrophication. Estuar Coast Shelf S 65: 239–252.

Gleitz M, Bartsch A, Dieckmann GS, Eicken H (1998) Composition and succession of sea ice diatom assemblages in the eastern and southern Weddell Sea, Antarctica. Antar Res S 73: 107–120.

Golden KM, Ackley SF, Lytle VI (1998) The percolation phase transition in sea ice. Science 282: 2238–2241.

Gosselin M, Levasseur M, Wheeler PA, Horner RA, Booth BC (1997) New measurements of phytoplankton and ice algal production in the Arctic Ocean. Deep-Sea Res Pt II 44: 1623–1644.

Granskog M, Kaartokallio H, Kuosa H, Thomas DN, Vainio J (2006) Sea ice in the Baltic Sea – A review. Estuar Coast Shelf S 70: 145–160.

Grossmann S, Gleitz M (1993) Microbial responses to experimental sea-ice formation: implications for the establishment of Antarctic sea-ice communities. J Exp Mar Biol Ecol 173: 273–289.

Gradinger R, Ikävalko J (1998) Organism incorporation into newly forming Arctic sea ice in the Greenland Sea. J Plant Res 20: 871–886.

Guillou L, Bachar D, Audic S, Bass D and others (2013) The Protist Ribosomal Reference database (PR2): a catalog of unicellular eukaryote Small Sub-Unit rRNA sequences with curated taxonomy. Nucleic Acids Res 41 D1: D597–D604.

Haecky P, Jonsson S, Andersson A (1998) Influence of sea ice on the composition of the spring phytoplankton bloom in the northern Baltic Sea. Polar Biol 20: 1–8.

Haecky P, Andersson A (1999) Primary and bacterial production in sea ice in the northern Baltic Sea. Aquat Microb Ecol 20: 107–118.

Hammer Ø, Harper DAT, Ryan PD (2001) PAST: Paleontological statistics software package for education and data Analysis. Palaeontol Electron 4: pp. 9.

HELCOM (1988) Guidelines for the Baltic monitoring programme for the third stage; Part D. Biological determinants. Balt Sea Environ Proc 27D: 16–23.

Hodal H, Falk-Petersen S, Hop H, Kristiansen S, Reigstad M (2012) Spring bloom dynamics in Kongsfjorden, Svalbard: nutrients, phytoplankton, protozoans and primary production. Polar Biol 35: 191–203.

Horn HS (1974) The ecology of secondary succession. Annu Rev Ecol Syst 5: 25–37.

Hugerth LW, Muller EEL, Hu YOO, Lebrun LAM and others (2014) Systematic Design of 18S rRNA Gene Primers for Determining Eukaryotic Diversity in Microbial Consortia. PLoS One 9: e95567.

Huson DH, Beier S, Flade I, Górska A and others (2016) MEGAN Community Edition - Interactive Exploration and Analysis of Large-Scale Microbiome Sequencing Data. PLoS Comput Biol 12(6): e1004957. doi:10.1371/journal.pcbi.1004957

Ikävalko J, Gradinger R (1997) Flagellates and heliozoans in the Greenland Sea ice studied alive using light microscopy. Polar Biol 17: 323−329.

631 Kaartokallio H (2004) Food web components, and physical and chemical properties of Baltic Sea
632 ice. Mar Ecol-Prog Ser 273: 49–63.

633 Kaartokallio H, Kuosa H, Thomas DN, Granskog MA, Kivi K (2007) Biomass, composition and
634 activity of organism assemblages along a salinity gradient in sea ice subjected to river discharge in
635 the Baltic Sea. Polar Biol 30: 183–197.

636 Kaartokallio H, Tuomainen J, Kuosa H, Kuparinen J and others (2008) Succession of sea-ice
637 bacterial communities in the Baltic Sea fast ice. Polar Biol 31: 783–793.

638 Kahru M, Savchuk OP, Elmgren R (2007) Satellite measurements of cyanobacterial bloom
639 frequency in the Baltic Sea: interannual and spatial variability. Mar Ecol-Prog Ser 343: 15–23.

640 Kangas P, Alasaarela E, Lax H-G, Jokela S, Storgård-Envall C (1993) Seasonal variation of primary
641 production and nutrient concentrations in the coastal waters of Bothnian Bay and The Quark. Aqua
642 Fenn 23: 165–176.

643 Klais R, Tamminen T, Kremp A, Spilling K and others (2013) Spring phytoplankton communities
644 shaped by interannual weather variability and dispersal limitation: Mechanisms of climate change
645 effects on key coastal primary producers. Limnol Oceanogr 58(2): 753–762.

646 Koroleff F (1976) Determination of nutrients. In Methods of Seawater Analysis. Grasshoff, K.
647 (eds.). Verlag Chemie, pp. 117–181.

648 Koskinen K, Hultman J, Paulin L, Auvinen P, Kankaanpää H (2011) Spatially differing bacterial
649 communities in water columns of the northern Baltic Sea. FEMS Microbiol Ecol 75: 99–110.

650 Kozich JJ, Westcott SL, Baxter NT, Highlander SK, Schloss PD (2013) Development of a dual-
651 index sequencing strategy and curation pipeline for analyzing amplicon sequence data on the MiSeq
652 Illumina sequencing platform. Appl Environ Microbiol 79: 5112–5120.

653 Krawczyk DW, Witkowski A, Juul-Pedersen T, Arendt KE and others (2015) Microplankton
654 succession in a SW Greenland tidewater glacial fjord influenced by coastal inflows and run-off
655 from the Greenland Ice Sheet. Polar Biol 38: 1515–1533.

656 Kremp A, Tamminen T, Spilling K (2008) Dinoflagellate bloom formation in natural assemblages
657 with diatoms: nutrient competition and growth strategies in Baltic spring phytoplankton. Aquat
658 Microb Ecol 50: 181–196.

659 Kuosa H, Autio R, Kuuppo P, Setälä O, Tanskanen S (1997) Nitrogen, Silicon and Zooplankton
660 controlling the Baltic spring bloom: An experimental study. Estuar Coast Shelf S 45: 813–821.

661 Legrand C, Fridolfsson E, Bertos-Fortis M, Lindehoff E and others (2015) Interannual variability of
662 phyto-bacterioplankton biomass and production in coastal and offshore waters of the Baltic Sea.
663 Ambio 44 (Suppl. 3): S427–S438.

664 Leu E, Mundy C, Assmy P, Campbell K and others (2015) Arctic spring awakening – Steering
665 principles behind the phenology of vernal ice algal blooms. Prog Oceanogr 139: 151–170.

666 Lips I, Rünk N, Kikas V, Meerits A, Lips U (2014) High-resolution dynamics of the spring bloom
667 in the Gulf of Finland of the Baltic Sea. J Marine Syst 129: 135–149.

668 Lizotte MP (2003) The microbiology of sea ice. In Sea Ice: An Introduction to Its Physics,
669 Chemistry, Biology and Geology. Thomas, D. N. and Dieckmann G. S. (eds.), Blackwell, Malden,
670 Mass, pp. 184–210.

671 Luhtala H and Tolvanen H (2013) Optimizing the Use of Secchi Depth as a Proxy for Euphotic Depth
672 in Coastal Waters: An Empirical Study from the Baltic Sea. ISPRS Int J Geoinf 2: 1153–1168.

673 Majaneva M, Rintala J-M, Hajdu S, Hällfors S and others (2012a) The extensive bloom of alternate-
674 stage *Prymnesium polylepis* (Haptophyta) in the Baltic Sea during autumn–spring 2007–2008. Eur J
675 Phycol 47: 310–320.

676 Majaneva M, Rintala J-M, Piisilä M, Fewer DP, Blomster J (2012b) Comparison of wintertime
677 eukaryotic community from sea ice and open water in the Baltic Sea, based on sequencing of the
678 18S rRNA gene. Polar Biol 35: 875–889.

679 Makarevich PR, Larionov VV, Moiseev DV (2015) Phytoplankton succession in the Ob-Yenisei
680 Shallow zone of the Kara Sea based on Russian databases. J Sea Res 101: 31–40.

681 Menden-Deuer S, Lessard EJ (2000) Carbon to volume relationships for dinoflagellates, diatoms,
682 and other protist plankton. Limnol Oceanogr 45: 569–579.

683 Meiners K, Vancoppenolle M, Thanassekos S, Dieckmann GS and others (2012) Chlorophyll a in
684 Antarctic sea ice from historical ice core data. Geophys Res Lett 39: L21602,
685 doi:10.1029/2012GL053478

686 Merkouriadi I, Leppäranta M (2014) Long-term analysis of hydrography and sea-ice data in
687 Tvärminne, Gulf of Finland, Baltic Sea. Climatic Change 124: 849–859.

688 Michel C, Legendre L, Therriault J-C, Demers S, Vandevelde T (1993) Springtime coupling
689 between ice algal and phytoplankton assemblages in southeastern Hudson Bay, Canadian Arctic.
690 Polar Biol 13: 441–449.

691 Mikkelsen DM, Rysgaard S, Glud RN (2008) Microalgal composition and primary production in
692 Arctic sea ice: a seasonal study from Kobbefjord (Kangerluarsunnguaq), West Greenland. Mar
693 Ecol-Prog Ser 368: 65–74.

694 Moreau S, Ferreyra GA, Mercier B, Lemarchand K and others (2010) Variability of the microbial
695 community in the western Antarctic Peninsula from late fall to spring during a low ice cover year.
696 Polar Biol 33: 1599–1614.

697 Nicolaus M, Katlein C, Maslanik J, Hendricks S (2012) Changes in Arctic sea ice result in
698 increasing light transmittance and absorption. Geophys Res Lett 39: L24501,
699 doi:10.1029/2012GL053738.

700 Niemi Å (1973) Ecology of phytoplankton in the Tvärminne area, SW coast of Finland I. Dynamics
701 of hydrography, nutrients, chlorophyll a and phytoplankton. Acta Bot Fenn 100: 1–69.

702 Niemi Å, Åström A-M (1987) Ecology of phytoplankton in the Tvärminne area, SW coast of
703 Finland. IV. Environmental conditions, chlorophyll *a* and phytoplankton in winter and spring 1984
704 at Tvärminne Storfjärd. Ann Bot Fenn 24: 333–352.

705 Niemi A, Michel C, Hille K, Poulin M (2011) Protist assemblages in winter sea ice: setting the
706 stage for the spring ice algal bloom. Polar Biol 34: 1803–1817.

Norrman B, Andersson A (1994) Development of ice biota in a temperate sea area (Gulf of Bothnia). Polar Biol 14: 531–537.

Olenina I, Hajdu S, Edler L, Andersson A and others (2006) Biovolumes and size-classes of phytoplankton in the Baltic Sea. Balt Sea Environ Proc 106: 1–144.

Padisák J, Soróczki-Pintér É, Rezner Z (2003) Sinking properties of some phytoplankton shapes and the relation of form resistance to morphological diversity of plankton – an experimental study. Hydrobiologia 500: 243–257.

Piiparinen J, Kuosa H, Rintala J-M (2010) Winter-time ecology in the Bothnian Bay, Baltic Sea: nutrients and algae in fast ice. Polar Biol 33: 1445–1461.

Popova EE, Yool A, Coward AC, Aksenov YK and others (2010) Control of primary production in the Arctic by nutrients and light: insights from a high resolution ocean general circulation model. Biogeosciences 7: 3569–3591.

Poulin M, Daugbjerg N, Gradinger R, Ilyash L and others (2011) The pan-Arctic biodiversity of marine pelagic and sea-ice unicellular eukaryotes: a first-attempt assessment. Mar Biodiv 41: 13–28.

Ratkova TN, Wassmann P, Verity PG, Andreassen IJ (1998) Abundance and biomass of pico-, nano-, and microplankton on a transect across Nordvestbanken, north Norwegian shelf, in 1994. Sarsia 84: 213–225.

Ratkova TN, Wassmann P (2005) Sea ice algae in the White and Barents seas: composition and origin. Polar Res 24: 95–110.

Riaux-Gobin C, Poulin M, Dieckmann G, Labrune C, Vétion G (2011) Spring phytoplankton onset after the ice break-up and sea-ice signature (Ade´lie Land, East Antarctica) Polar Res 30, 5910, doi: 10.3402/polar.v30i0.5910

Riedel A, Michel C, Gosselin M, LeBlanc B (2008) Winter–spring dynamics in sea-ice carbon cycling in the coastal Arctic Ocean. J Marine Syst 74: 918–932.

Rintala J-M, Piiparinen J, Uusikivi J (2010) Drift-ice and under-ice water communities in the Gulf of Bothnia (Baltic Sea). Polar Biol 33: 179–191.

Rintala J-M, Piiparinen J, Blomster J, Majaneva M and others (2014) Fast direct melting of brackish sea-ice samples results in biologically more accurate results than slow buffered melting. Polar Biol 37: 1811–1822.

Różańska M, Poulin M, Gosselin M (2008) Protist entrapment in newly formed sea ice in the Coastal Arctic Ocean. J Marine Syst 74: 887–901.

Różańska M, Gosselin M, Poulin M, Wiktor JM, Michel C (2009) Influence of environmental factors on the development of bottom ice protist communities during the winter-spring transition. Mar Ecol-Prog Ser 386: 43–59.

Sildever S, Andersen TJ, Ribeiro S, Ellegaard M (2015) Influence of surface salinity gradient on dinoflagellate cyst community structure, abundance and morphology in the Baltic Sea, Kattegat and Skagerrak. Estuar Coast Shelf S 155: 1–7.

Sildever S, Kremp A, Enke A, Buschmann F and others (2017) Spring bloom dinoflagellate cyst dynamics in three eastern sub-basins of the Baltic Sea. Cont Shelf Res 137: 46–55.

Sime-Ngado T, Gosselin M, Juniper SK, Levasseur M (1997) Changes in sea-ice phagotrophic microprotists (20–200 µm) during the spring algal bloom, Canadian Arctic Archipelago. J Marine Syst 11: 163–172.

Smith WO, Brightman RI, Booth BC (1991) Phytoplankton biomass and photosynthetic response during the winter-spring transition in the Fram Strait. J Geophys Res-Oceans 96: 4549–4554.

Sommer U, Gliwicz ZM, Lampert W, Duncan A (1986) PEG-model of Seasonal Succession of Planktonic Events in Fresh Waters. Arch Hydrobiol 106: 433–471.

Sommer U, Aberle N, Engel A, Hansen T and others (2007) An indoor mesocosm system to study the effect of climate change on the late winter and spring succession of Baltic Sea phyto- and zooplankton. Oecologia 150: 655–667.

Stoecker DK, Buck KR, Putt M (1992) Changes in the sea-ice brine community during the spring-summer transition, McMurdo Sound, Antarctica. I. Photosynthetic protists. Mar Ecol-Prog Ser 84: 265–278.

Stoecker DK, Buck KR, Putt M (1993) Changes in the sea-ice brine community during the spring-summer transition McMurdo Sound, Antarctica. II. Phagotrophic protists. Mar Ecol-Prog Ser 95: 103–113.

Stoecker DK, Gustafson DE, Black MMD, Baier CT (1998) Population dynamics of microalgae in the upper land-fast sea ice at a snow-free location. J Phycol 34: 60–69.

Sukhanova IN, Flint MV, Pautova LA, Stockwell DA and others (2009) Phytoplankton of the western Arctic in the spring and summer of 2002: Structure and seasonal changes. Deep-Sea Res Pt II 56: 1223–1236.

Svedén JB, Walve J, Larsson U, Elmgren R (2016) The bloom of nitrogen-fixing cyanobacteria in the northern Baltic Proper stimulates summer production. J Marine Syst 163: 102–112.

Syvertsen EE (1991) Ice algae in the Barents Sea: types of assemblages, origin, fate and role in the ice-edge phytoplankton bloom. Polar Res 10: 277–287.

Tansley AG (1935) The use and abuse of vegetational concepts and terms. Ecology 16: 284–307.

Tilman D (1982) Resource competition and community structure. Monographs in Population Biology. Princeton University Press, Princeton, New Jersey.

Tuschling K, v Juterzenka K, Okolodkov YB, Anoshkin A (2000) Composition and distribution of the pelagic and sympagic algal assemblages in the Laptev Sea during autumnal freeze-up. J Plant Res 22: 843–864.

Thomson PG, McMinn A, Kiessling I, Watson M, Goldsworthy PM (2006) Composition and succession of dinoflagellates and chrysophytes in the upper fast ice of Davis Station, East Antarctica. Polar Biol 29: 337–345.

Ulanova A, Busse S, Snoeijs P (2009) Coastal diatom-environment relationships in the brackish Baltic Sea. J Phycol 45: 54–68.

Ütermöhl H (1958) Zur Vervollkommnung der quantitativen Phytoplankton-Methodik. Mitteilungen Internationale Vereinigung für Theoretische und Angewandte Limnologie 9: 1–38.

Wasmund N, Voss M, Lochte K (2001) Evidence of nitrogen fixation by non-heterocystous cyanobacteria in the Baltic Sea and re-calculation of a budget of nitrogen fixation. Mar Ecol-Prog Ser 214: 1–14.

Winder M, Berger SA, Lewandowska A, Aberle N and others (2012) Spring phenological responses of marine and freshwater plankton to changing temperature and light conditions. Mar Biol 159: 2491–2501.

Zhang Z, Schwartz S, Wagner L, Miller W (2000) A greedy algorithm for aligning DNA sequences. J Comput Biol 7: 203–214.

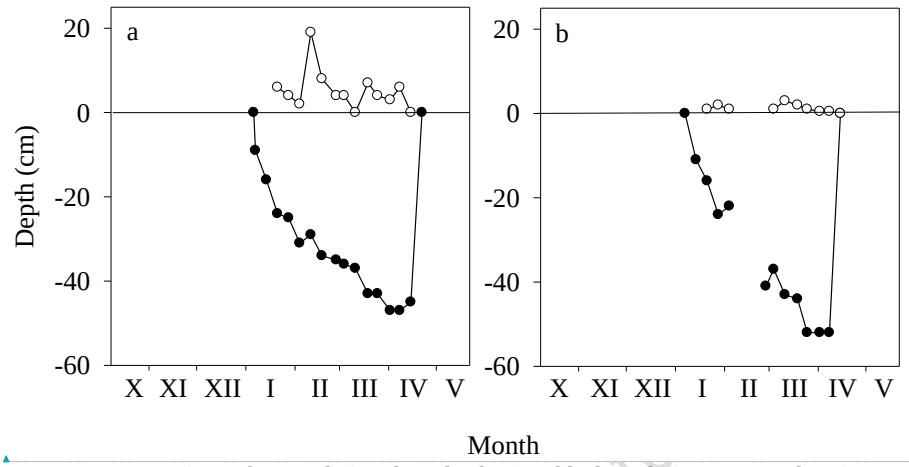

Field Code Changed

Fig. 1 Mean snow (cm, white circles) and ice depths (cm, black circles) at Krogarviken (site A, a) and Storfjärden (site B, b). Depth of 0 cm denotes the ice surface.

799

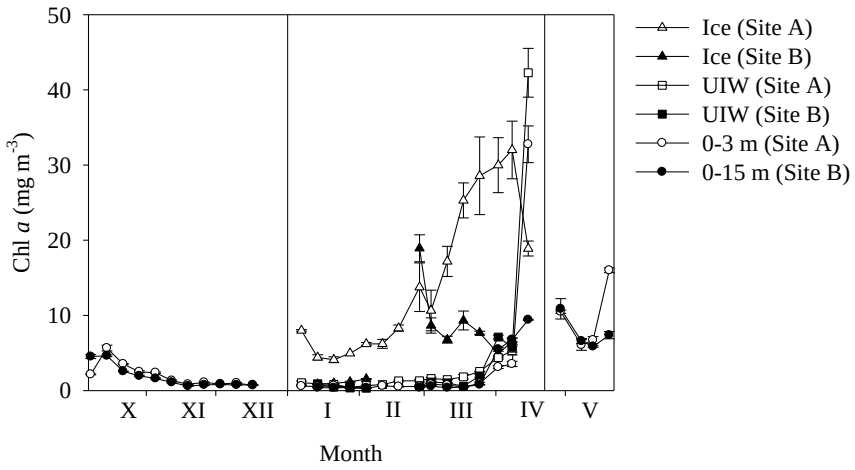

Fig. 2 The chl *a* concentration (mean ± sd, mg chl *a* m^{-3}) throughout the cold-water season from the beginning of October until the end of May in ice, under-ice water (UIW) and the 0–3-m layer at Krogarviken (site A, open symbols) and in ice, UIW and the 0–15-m layer at Storfjärden (site B, filled symbols). The timeline from the beginning of January to the end of April represents the ice-covered season.

807

808

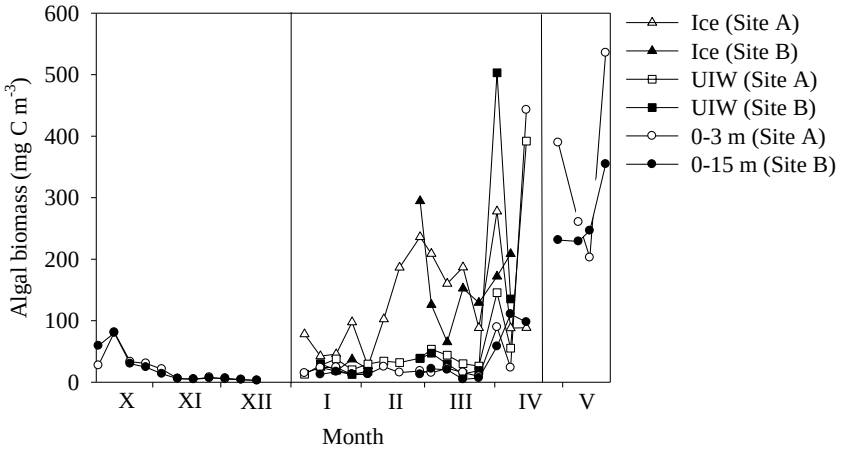

Fig. 3 Total algal biomass (mg C m^{-3})

816 throughout the cold-water season from the beginning of October until the end of May in ice, under-
817 ice water (UIW) and the 0–3-m layer at site A (open symbols) and in ice, UIW and the 0–15-m
818 layer at site B (filled symbols). The timeline from the beginning of January to the end of April
819 represents the ice-covered season.

820

Fig. 4

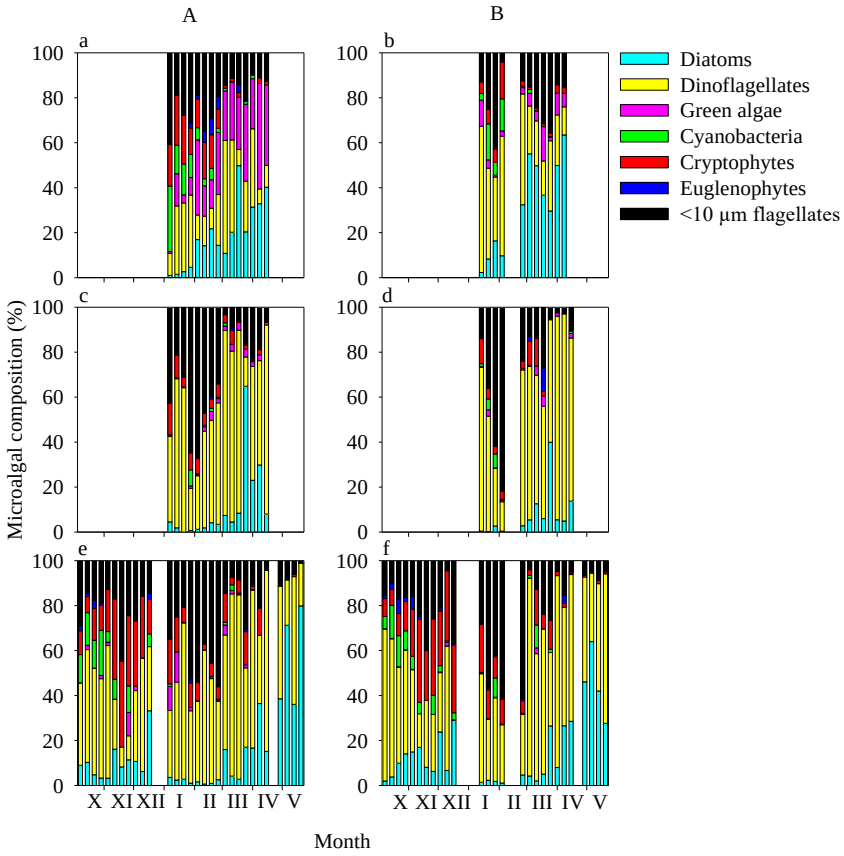

822 Seasonal succession of the microalgal assemblage composition (% of the total biomass) in ice (a, b),
823 under-ice water (UIW; c, d), the 0–3-m layer (e) and 0–15-m layer at Krogarviken (A) and
824 Storfjärden (B), October–May.

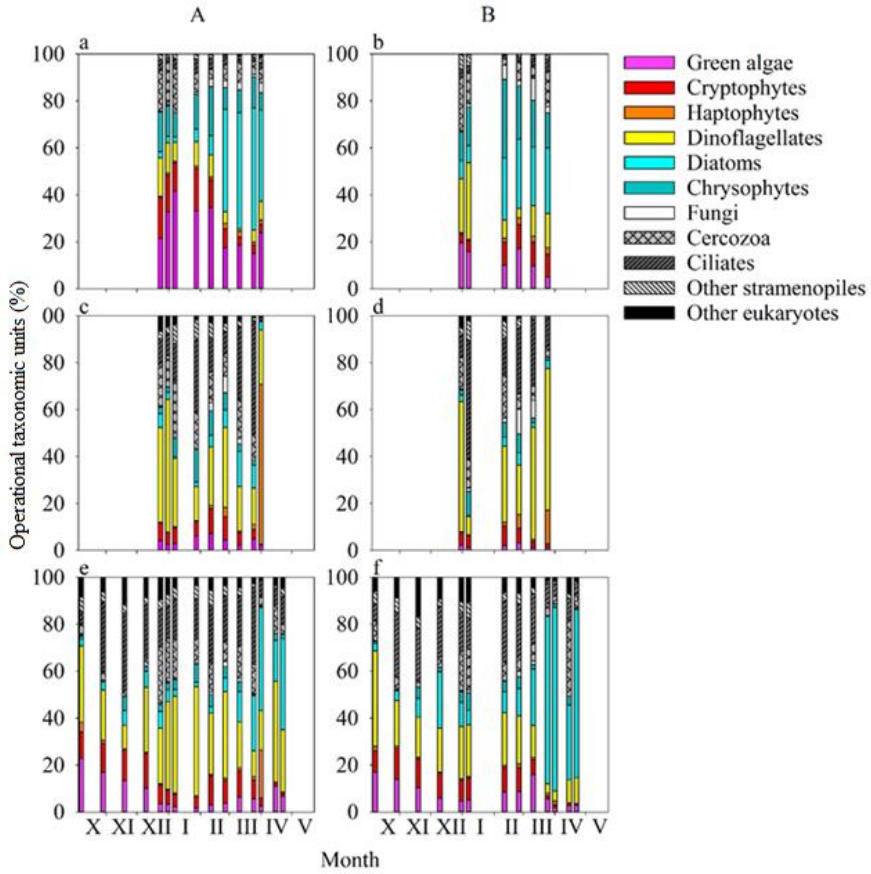

825
826 Fig. 5 Seasonal succession of the operational taxonomic units (OTU) composition (% of the total
827 OTUs) in ice (a, b), under-ice water (UIW; c, d), the 0–3-m layer (e) and 0–15-m layer at
828 Krogarviken (A) and Storfjärden (B), October–May.

Fig. 6

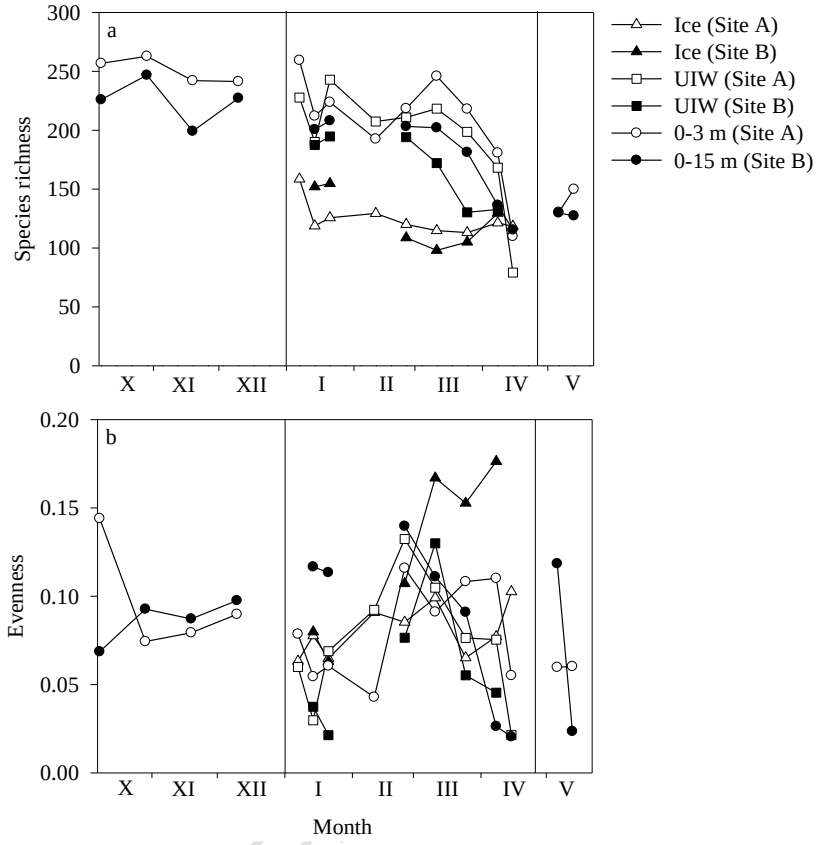

830 Comparison of richness (a) and evenness (b) throughout the cold-water season from the beginning
831 of October until the end of May in ice, under-ice water (UIW) and the 0–3-m layer at site A (open
832 symbols) and in ice, UIW and the 0–15-m layer at site B (filled symbols). The timeline from the
833 beginning of January to the end of April represents the ice-covered season.

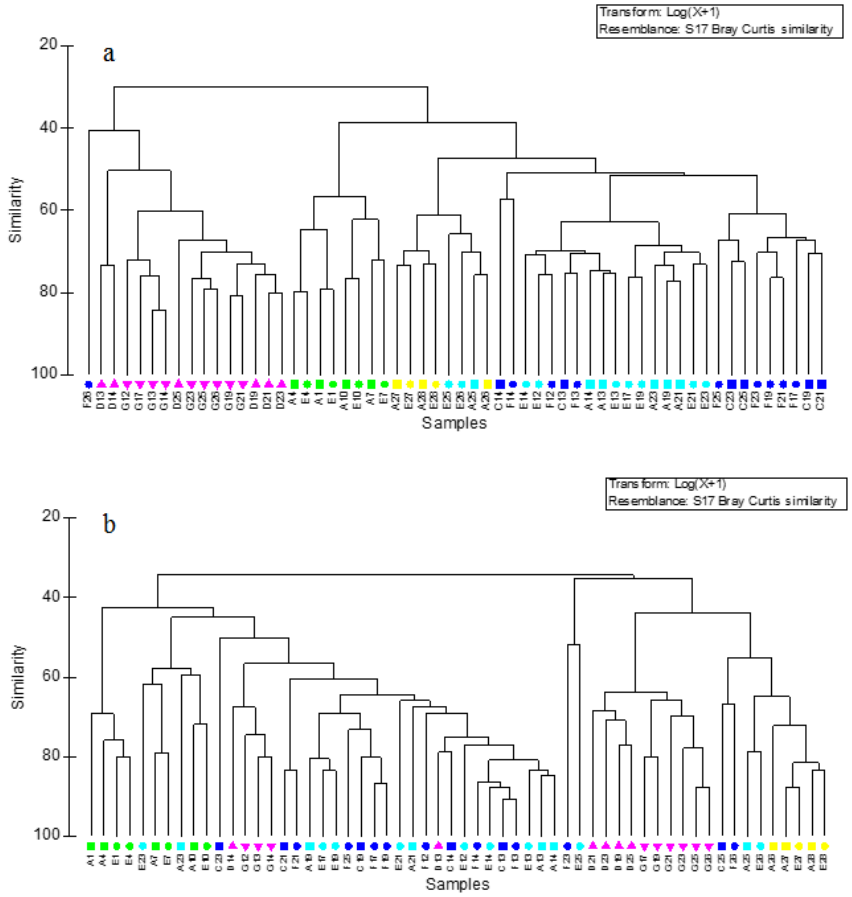

834

835 Fig. 7 Dendrograms for percent similarity produced from the Bray-Curtis similarities for OTUs (a)
836 and the microscopy results (b).

	A	B
Fall	●	■
Winter	●	■
UIW	●	■
Ice	▼	▲
Spring	●	■

837